Effects of Engine Exhaust Flow on Boattail Drag

DAVE BERGMAN*
Convair Aerospace Division of General Dynamics Corporation, Fort Worth, Texas

Wind-tunnel tests were conducted to investigate the effects of jet plume shape and entrainment on boattail pressure drag. The results were used to determine nozzle drag levels at various engine operating conditions as well as at conditions related to airplane force models. An isolated nozzle model with a pressure-tapped exterior and changeable internal parts was tested subsonically to examine changes in drag due to alterations in internal geometry and nozzle pressure ratio. In addition, tests were run with solid plume-shaped sleeves as a means to separate plume-shape effects from jet entrainment effects. Large differences in drag were measured with changes in plume shape, and, in certain regimes, jet entrainment also had a significant effect. The results of this study include boattail pressure distributions, integrated drag coefficients, and a comparison of test data with analytically predicted drag levels.

Nomenclature

A = cross-sectional area
C_D = boattail pressure drag coefficient (drag/q_0A_m)
C_P = boattail pressure coefficient $[(P - P_0)/q_0]$
D,d = diameter
h = boundary-layer height
L = length of boattail
M_0 = freestream Mach number
NPR = nozzle pressure ratio (P_{TJ}/P_0)
P = local static pressure
P_0 = freestream static pressure
P_{TJ} = exhaust jet total pressure
q = dynamic pressure
R = radius
β = boattail trailing-edge angle

Subscripts

B,b = boattail terminal plane
J = jet
M,m = maximum
0 = freestream
T = total

I. Introduction

COMPREHENSIVE engine-airframe integration is essential in the design of advanced aircraft. In a real sense, this area concerns each of the many systems which concurrently affect both the engine and airframe; however, the context in which engine-airframe integration will be discussed here is limited to that of aerodynamic interactions. In particular, attention is directed to the engine exhaust nozzle, where significant internal-external flow interactions exist.

The engine nozzle is normally an exposed portion of the airframe; thus its external performance (i.e., "boattail" drag), in addition to the performance of other nearby structure, is affected by engine exhaust flow. Therefore, insight into nozzle-generated flowfields becomes a valuable aid in detecting potentially good or bad installations while an aircraft is still in the preliminary design phase.

Problem Statement

Nozzle boattail drag can amount to a sizeable percentage of over-all airplane drag (15% is not uncommon). These levels vary widely, depending upon boattail geometry and the local flowfield created by both the fuselage and the engine exhaust. Concern over nozzle drag is brought about by the large aft-facing projected areas that exist while a nozzle is in a closed, "dry power" position used in subsonic flight. Otherwise, for supersonic flight, the nozzle opens for an afterburning or "reheat" position and, as illustrated in Fig. 1, the nozzle then has relatively little projected area.

Much work has been done to develop low-drag boattail shapes for high subsonic Mach numbers. Results show that, for a given fineness ratio, a circular-arc shape provides a relatively small amount of pressure drag.[1] In comparison, the drag of a conical shape is quite large, as is seen in Fig. 2. The flowfield across a conical boattail is characterized by rapid flow expansion at the sharp-edged corner. By smoothing the transition, as done with the circular arc, less flow expansion occurs, thereby reducing momentum losses and lowering drag. With this in mind, the problem arises as to what are the effects of various exhaust jet conditions on a smoothly contoured boattail. The difficulty in handling the problem analytically is that jet effects are actually functions of several interactions, including such parameters as nozzle pressure ratio (ratio of jet total pressure to freestream static pressure), real-gas effects, the particular exhaust flow direction (nozzles with centerbody plugs), and the amount of jet-induced flow entrainment that is created. These complicated flow interactions emphasize the need for using experimental as well as analytical means to examine boattail flowfields.

In addition to analyzing boattail drag with regard to engine operation, there is another area of concern: the simulation of jet effects without the use of pressurized exhaust flow. Many airplane wind-tunnel models cannot provide high-pressure exhaust jets; thus a technique for artificially creating jet effects is desirable. One way to attempt simulation of jet flow is to add a solid, plume-shaped extension to the nozzle. Even assuming that extensions can be designed to at least approximate the actual plume shape, the extensions cannot reproduce jet entrainment effects; therefore, the validity of this method additionally depends upon the significance of entrainment.

Method of Approach

Experimenters have recorded changes in boattail drag with variations in parameters such as nozzle pressure ratio, but the two basic components of the jet effect, jet plume shape and jet entrainment, are usually measured together as an over-all net effect. As a consequence, the significance of each component is hidden. If, instead, there were more comprehensive data as to what causes jet effects to differ

Presented as Paper 70-132 at the AIAA 8th Aerospace Sciences Meeting, New York, January 19–21, 1970; submitted February 19, 1970; revision received April 1, 1970.

* Propulsion Engineer, Aerospace Technology Department.

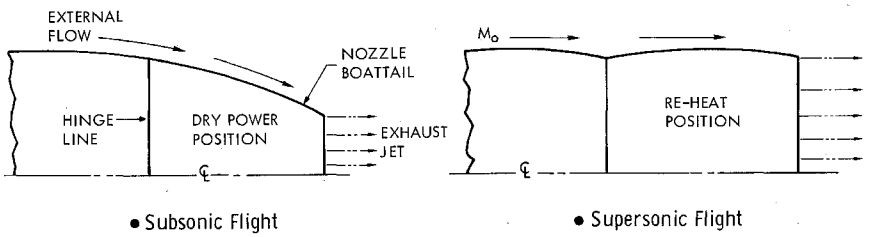

Fig. 1 Exhaust nozzle positions.

with changing exhaust conditions, boattail drag analyses could be made more accurate.

The approach taken here is to evaluate each of the jet-effect components as well as to examine the net effect. This is done by 1) measuring boattail drag without jet flow and then comparing this drag to the drag with a solid, plume-shaped extension attached, with the resultant drag difference being denoted as plume-shape effect, and 2) measuring boattail drag with a solid extension attached and then comparing this drag to the drag without the extension but with pressurized exhaust flow in its place. This difference in drag is denoted as jet entrainment effect. This technique is presented pictorially in Fig. 3.

With the preceding goals in mind, a series of wind-tunnel tests were conducted. A conical plug-type nozzle, representative of dry-power mode for subsonic flight, was chosen as the baseline model. A unique design feature of the model is interchangeable internal geometry for accommodating several different centerbody plugs as well as solid sleeve extensions. In this manner, the effects of changes in internal geometry could be investigated while retaining the identical boattail.

Since the test was meant to obtain a general description of boattail flowfields, the nozzle model was tested isolated rather than installed in a particular aircraft configuration. Therefore, the results can be used as a general guideline to precede analyses with specific airframes in mind.

The exhausts considered were 1) conical plug nozzle flow, 2) convergent nozzle flow, and 3) an exhaust typical of airplane "force" models. Airplane force models are used to determine lift, drag, and moment forces. In the process, flow-through nacelles take the place of engine packages. Unlike engine nozzles, the force model counterpart has low-pressure exhausts and, in addition, is usually partially plugged to set inlet mass flow to the desired conditions.

II. Model Test Technique

The nozzles were tested at several subsonic freestream Mach numbers and through a range of nozzle pressure ratios. Boattail drag measurements were made by instrumenting the model with static pressure orifices. Data from the orifices were used to determine boattail pressure distribution and, when integrated over the projected area, provided boattail pressure drag.

Specifically, tests were conducted at Mach numbers of 0.55, 0.70, and 0.85, while nozzle exhaust flow ranged from jet-off to a pressure ratio of 4. Nozzle centerbodies were alternately changed to simulate a conical plug nozzle, force model nozzle, and a nozzle with axially directed convergent flow. The models were nonejector types; thus, there were no secondary flows. All configurations retained the minimum internal flow area at the nozzle exit plane. In order to accomplish this for the convergent-type nozzle, it was necessary to use a long, axial, centerbody extension. It is felt from the results that adequate simulation of convergent nozzle flow was accomplished by this means.

It is important to note that the fixed boattail shape was designed for the baseline plug nozzle; therefore, a convergent nozzle with equivalent jet area and thrust would require a smaller nozzle exit diameter. However, axially directed nozzle flow was simulated only to investigate the effects of varying jet direction rather than to determine the relative merits of one nozzle type over another.

The jet plume shape for a convergent nozzle with a fully expanded flow ($NPR \approx 2$) was simulated by a long, cylindrical sleeve. A typical cruise condition for a plug-type nozzle usually approximates a pressure ratio of 3; thus, the plume shape for the plug nozzle at an NPR of 3 was predicted and used to define a sleeve extension. As the result of assuming an isentropic flow expansion from the nozzle exit to the end of the plug, a truncated conical sleeve design was used for plug nozzle plume simulation.

Description of Test Facilities

Tests were conducted in a freejet wind tunnel at the Convair Aerospace Division. A schematic of the tunnel is presented in Fig. 4. Ambient air, which is first drawn into a bellmouth inlet, flows through a smaller, square-shaped channel that connects to a large plenum chamber. It is at this point that a freejet test section is formed. Located here, the model becomes surrounded by high-velocity freestream flow. Various tunnel pressure data are measured by a scanivalve system and then reduced into final form by an on-line computer.

A hollow pipe of circular cross section is used both to support the model and to deliver pressurized nozzle flow. Total pressure surveys of the pipe show a turbulent boundary layer with a height equal to approximately 17% of the model diameter ($h/d_m \approx 0.17$) at the nozzle connect point. This approximates the boundary-layer thickness for a fuselage in-

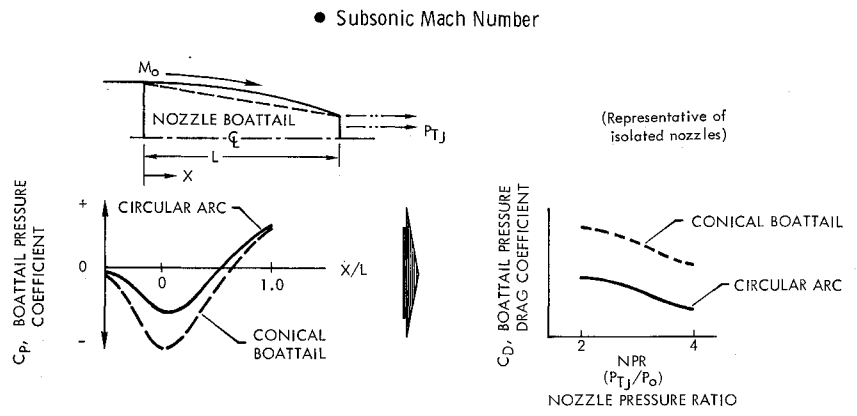

Fig. 2 Typical boattail flow properties.

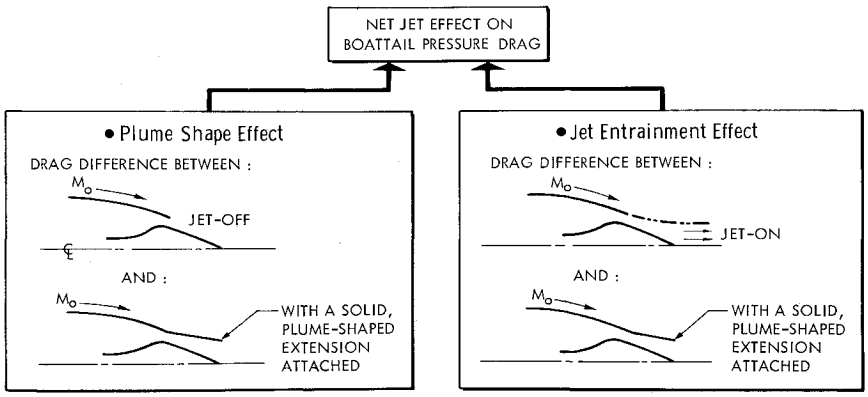

Fig. 3 Determining the components of jet effect.

stallation, whereas a pod-type nozzle mounting would normally involve less boundary-layer growth.

Model and Instrumentation

A 3-in.-diam nozzle with a circular-arc boattail was used along with several centerbody plugs and sleeve extensions. Geometry of the parts is shown in Fig. 5. Note that the force-model plug is much smaller than the conical plug, and, in addition, is truncated at the nozzle exit. The force-model

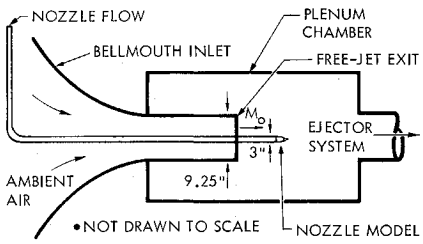

Fig. 4 Schematic of the freejet wind tunnel.

plug is sized relative to setting a typical inlet massflow. Truncation of the force-model plug on airplane models is done so that plug drag can easily be measured apart from over-all airplane drag by relatively few base pressure taps. This truncated plug was retained for the present tests only for the purpose of duplicating a typical force-model geometry.

As shown in Fig. 5, the force-model plug was extended aft of the boattail in order to create an axial flow condition similar to convergent nozzle flow.

Two sleeve extensions were used as plume-shape simulators: a cylindrical sleeve to simulate fully expanded convergent nozzle flow at $NPR \approx 2$ and a truncated conical sleeve to represent plug nozzle flow at $NPR \approx 3$.

Centerbody plugs were attached to an internal strut support by means of a threaded connection, while the sleeve extensions were slid into place and locked by set-screws. Model internal instrumentation included three strut-mounted total-pressure tubes for determining nozzle pressure ratio. The external boattail surface contained 30 static pressure orifices distributed along four rows separated by 90° quadrants. The location of the various instrumentation is shown in Fig. 6.

III. Results

The boattail configuration with the long cylindrical extension is similar to a model tested by NASA/Lewis.[1] Consequently, a comparison was made between General Dynamics and NASA/Lewis boattail pressure data. The results, given in Fig. 7, show excellent agreement both in level and trend.

Plots of boattail pressure coefficient C_p vs the ratio of local to maximum cross-sectional area A/A_m are presented in Fig. 8. With this type of plot, the integral beneath the curve defines the boattail drag coefficient. Although each of the pressure distributions have typical boattail flow expansion-compression trends, it is evident that changes in exhaust conditions had considerable effects on pressure levels. For example, the nozzle with the conical plug imparted only partial boattail flow recompression as opposed to the convergent nozzle.

For purposes of comparison with test data, an analytical boattail pressure drag was calculated for the convergent nozzle

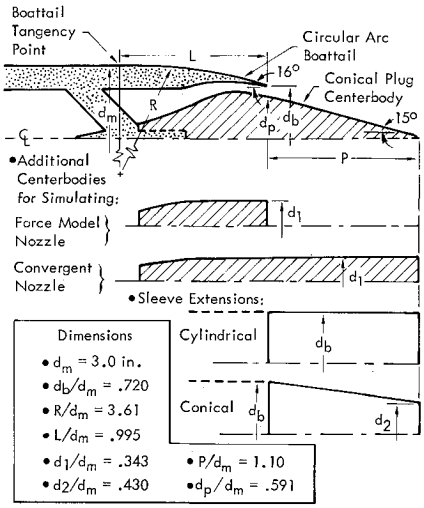

Fig. 5 Nozzle geometry.

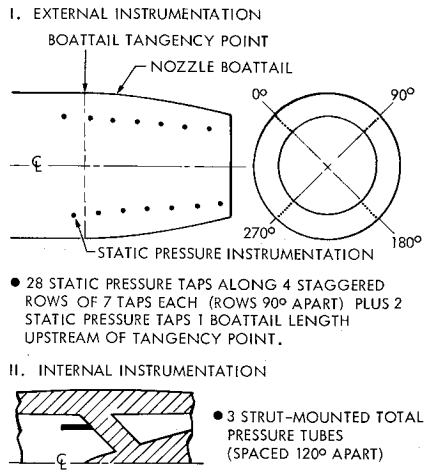

Fig. 6 Model instrumentation.

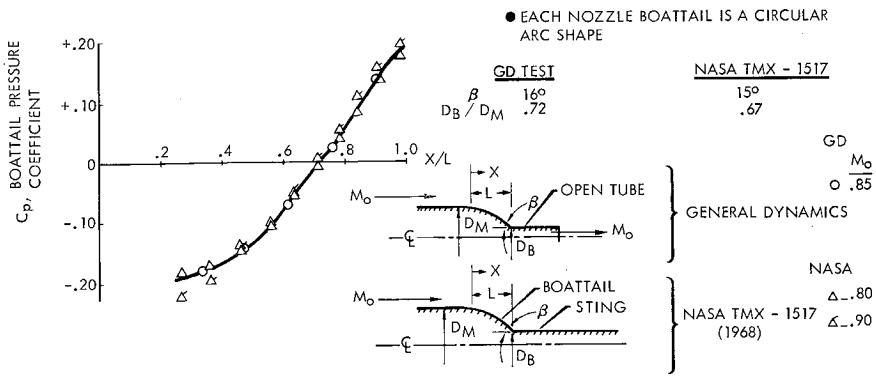

Fig. 7 Data substantiation.

and is shown in Fig. 9. The analytical procedure involved a method-of-characteristics solution to define jet plume shape, and a transonic flow calculation to define boattail pressures. The combination of these two methods plus a correction for boundary-layer thickness resulted in significantly less drag than that of the measured data. However, the calculations did not account for jet entrainment.

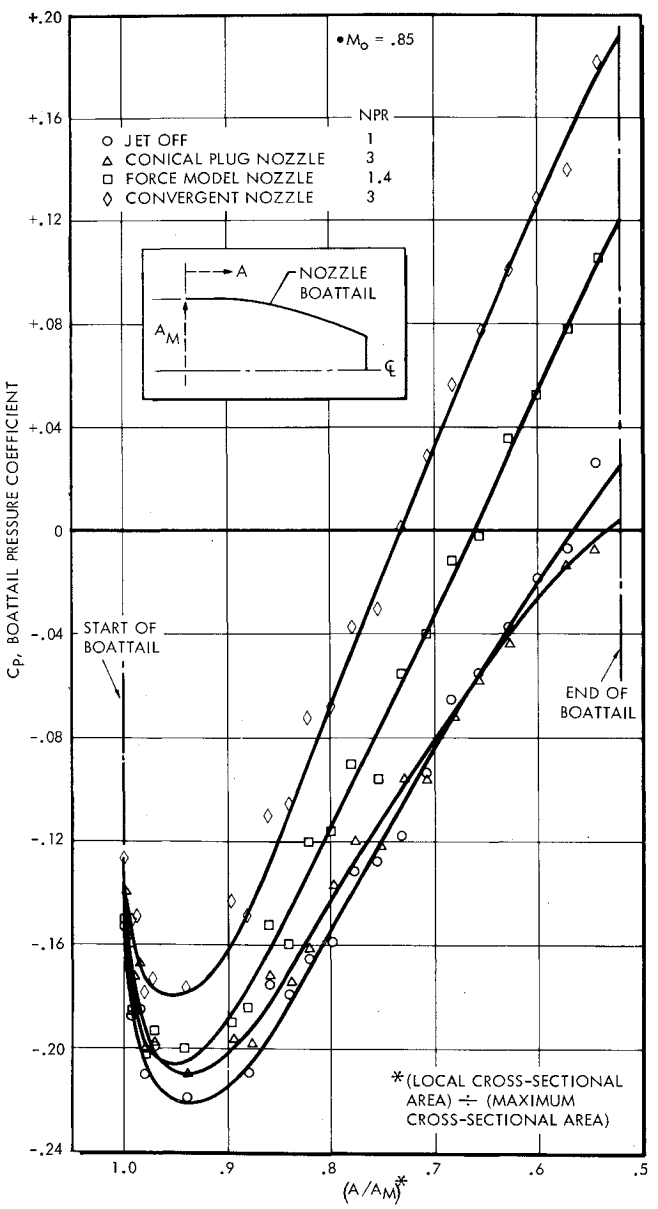

Fig. 8 Effects of exhaust flow on boattail pressure distribution.

Plots of boattail pressure drag coefficient C_D vs nozzle pressure ratio NPR are given in Fig. 10. Both the plug and convergent nozzles exhibit similar drag trends but different drag levels. After jet flow is initiated, boattail drag first decreases until nozzle jet velocity approximates that of the surrounding flow, wherein drag then increases until the just-choked condition ($NPR \approx 2$) is attained. Further increases in pressure ratio result in another downward drag trend. The drag level with the conical plug nozzle remains much larger at all conditions that that with either the force model plug or the convergent nozzle configurations. The force-model nozzle, with operational jet flow limited to low-pressure ratios, has drag levels between those of the conical plug and convergent nozzles.

The drag level with the sleeve extension remains essentially constant with changes in nozzle flow. The cylindrical sleeve produces the least boattail drag of all the configurations tested except for the convergent nozzle at pressure ratios above 3.

Because the tests were conducted at several freestream Mach numbers, it was possible to obtain some information concerning drag-rise characteristics. Boattail drag coefficient for the conical plug nozzle is presented in Fig. 11 as a function of Mach number. With the jet off, a drag rise has taken place at Mach 0.85; however, at typical jet-on conditions, drag rise is delayed such that at Mach 0.85 and a pressure ratio of 3 the drag coefficient remains practically the same as at Mach 0.55 and 0.70.

The bar chart in Fig. 12 is an illustration of the significant difference between force model drag and the drag of high-pressure-ratio nozzles with identical external contours. The force model nozzle does not match the drag of either the plug or convergent nozzles. The force-model pressure ratio was taken to be at a 90% freestream recovery factor, which is typical for flow-through nacelles.

Figure 13 contains the results of dividing net jet effect into components by use of the solid-sleeve extensions. It is

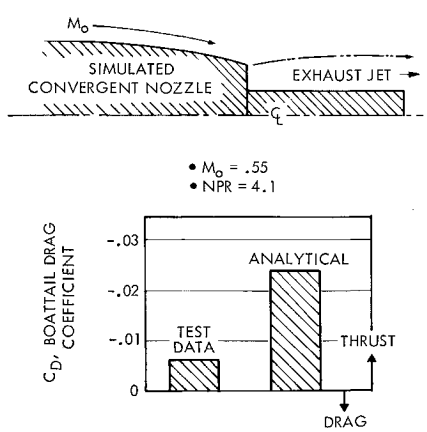

Fig. 9 Comparison between test data and analytical results.

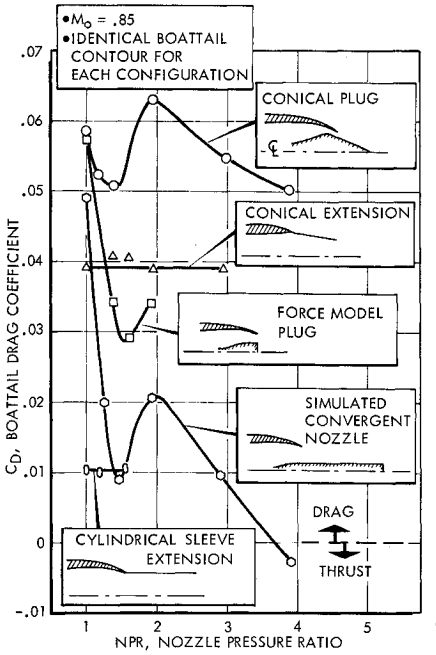

Fig. 10 Effects of exhaust flow on boattail drag.

evident that both the jet entrainment and the plume-shape effects were significant for the configurations tested.

IV. Analysis

The results in Fig. 13 were used to construct a general description of jet effects, as shown in Fig. 14. Because of the extrapolation involved, the curves in Fig. 14 are meant to depict a qualitative rather than a precise quantitative description. Jet entrainment is shown to begin its effect on boattail drag at a jet velocity approximating freestream velocity and then to gain in strength with increasing pressure ratio. This effect is continuously detrimental since jet entrainment creates an induced speed-up of boattail flow, which lowers boattail pressures. In contrast, the jet plume-shape effect is shown as continuously beneficial since it acts to move boattail flow streamlines away from the centerline, thereby causing stronger flow recompression on the boattail surface as compared to jet-off conditions.

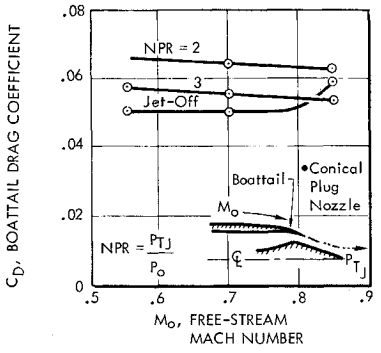

Fig. 11 Boattail drag rise characteristics.

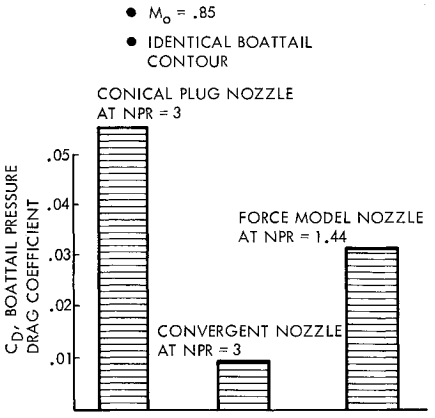

Fig. 12 Nozzle drag comparison.

The jet plume is unable to "billow out" beyond the exit area until a sonic exit is established, thus the plume-shape effect is assumed to be virtually constant from a jet velocity equal to freestream to a just-choked exit. As nozzle pressure ratio is increased past the just-choked condition ($NPR \approx 2$), the plume expands and its effect on drag becomes more pronounced by causing further displacement of boattail flow streamlines. The net, combined effect of jet entrainment and plume shape shown in Fig. 14 results in the same general trends for both the plug and convergent nozzles.

Larger levels of drag with the conical plug nozzle relative to the convergent nozzle can be explained by differences in plume shape. The plug nozzle plume causes boattail flow to be turned axial downstream of the boattail surface rather than to force an earlier recompression at the boattail end as caused by the convergent nozzle flow. As a result, boattail pressures with the conical plug remain relatively low, while flow recompression occurs downstream, adjacent to the plug.

The force model nozzle typically operates at nozzle pressure ratios low enough for the nozzle to be void of any jet entrainment or plume billowing effects. In addition, force-model boattail drag is unlike the drag of the other nozzles tested because of the flat base of the plug. The force-model exhaust fills the separated base region in a manner that distorts the plume shape relative to engine nozzles.

As expected, the sleeve extensions caused considerable turning of the boattail flow compared to jet-off and sleeve-off conditions. As seen in Fig. 10, the conical sleeve produces more boattail drag than does the cylindrical sleeve because of less boattail flow recompression. However, neither of the sleeves reproduces the engine nozzle jet effects at the pressure

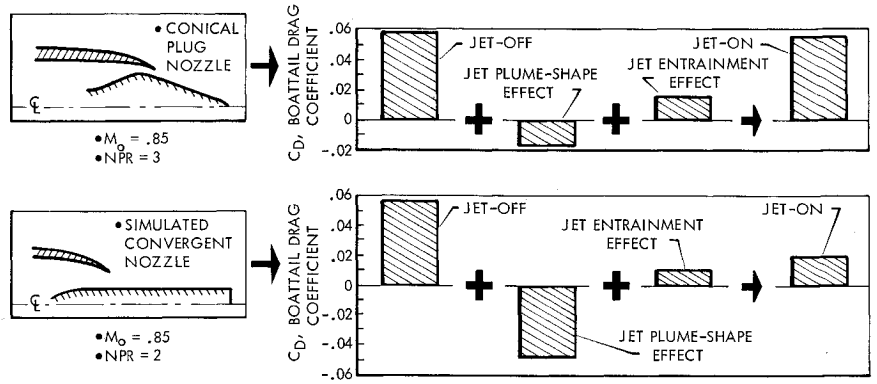

Fig. 13 Components of the jet effect.

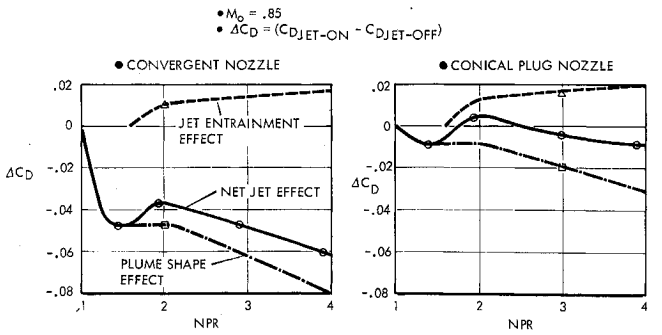

Fig. 14 General trends of jet effects.

ratios for which they are designed. This is due to their inability to simulate jet entrainment effects.

V. Conclusions

The following conclusions are made for the configurations tested.

1) Flow entrainment caused by the exhaust jet affects boattail flow significantly. This may, in part, explain why experimenters have had only varying success in duplicating jet effects with solid, plume-shaped extensions. Solid extensions may adequately simulate exhaust jets which entrain relatively little external flow as, for example, can be the case in ejector-type nozzles.[2] Since an ejector nozzle pumps internal secondary flow, its ability to entrain boattail flow is diminished. However, as seen in the General Dynamics tests, jet entrainment of the nonejector nozzles tested readily affects boattail flow whereas solid extensions do not reproduce this effect.

2) The boattail tested has three to four times more drag with conical plug exhaust flow than with axially directed convergent flow. This illustrates the strong effect of plume shape on boattail flowfield.

3) Drag levels on the typical force-model nozzle are misleading. The flow-through-nacelle nozzle tested exhibits different drag levels than do counterpart engine nozzles. This result is explained by particular differences in plume shape and entrainment effects.

References

[1] Shrewsbury, G. D., "Effect of Boattail Juncture Shape on Pressure Drag Coefficients of Isolated Afterbodies," TM X-1517, March 1968, NASA.

[2] Harrington, D. E., "Jet Effects on Boattail Pressure Drag of Isolated Ejector Nozzles at Mach Numbers from 0.60 to 1.47," TM X-1785, May 1969, NASA.

JUNE 1971 J. AIRCRAFT VOL. 8, NO. 6

Combined Inertial—ILS Aircraft Navigation Systems

JAMES W. BURROWS*
The Boeing Company, Seattle, Wash.

Error models for the Instrument Landing System (ILS) and Inertial Navigation System (INS) are discussed. A method for combining the two systems using the theory of optimal linear estimation is given. Results of tests of the combined navigation system using a ground vehicle operating on runways and instrumented with an inertial navigator, radio receivers, and a computer, are given with emphasis on the effects of initialization and unmodeled errors. The results indicate that use of the combined system during landing approach would simultaneously reduce the cross-runway position and velocity (track angle) errors. The combined system is relatively insensitive to the choice of initial values of certain parameters. Results are still good when the initial parameter values are chosen to approximate a real-time least square fit of INS position and velocity to the ILS localizer signal. The effects of the principal unmodeled error, platform tilt, are such that the tilt would have to be precorrected or included in the error model during approach if a poorer INS were to be employed.

Instrument Landing System (ILS) and Its Errors

SINCE its development just before World War II, the ILS has become the principal method of aircraft navigation during final approach to a landing at larger airports in bad weather. As of the beginning of 1969, there were 377 ILS installations in the United States, and probably that many again in the rest of the world. The principal component of the system is the localizer, which provides lateral course information. It consists of two directional antennas whose patterns are symmetrically placed with respect to the runway centerline. The carrier from one is modulated with a 90-Hz tone, and the other with 150 Hz. The aircraft localizer receiver compares the output of two audio filters centered on the modulation frequencies. The output of the receiver should be proportional to the angle from the aircraft to the runway centerline at the localizer antenna. Additional components of the ILS are the glide slope for descent information, marker beacons and compass locators for range information, and last, but not least, approach lights.[1]

The output of the localizer receiver usually varies from the above proportionality relationship. It has long been recognized that these errors are due to radiation scattering from objects illuminated by the localizer transmitter.[2] Indeed, a plot of the localizer receiver output along the runway

Received October 8, 1969; revision received February 24, 1970. The author wishes to thank the staff of the Automatic Flight Management Laboratory of The Boeing Commercial Airplane Division for their devoted labor during the tests reported in this paper, particularly G. Hadley, who programed most of the real time and post-run computations.

* Senior Specialist Engineer, Mathematical Sciences, Aerospace Group.